Synthesis and Thermally and Light Driven Cleavage of an N-Heterocyclic Diphosphine with Inorganic Backbone

Blum, Markus

2021-02-24

Blum , M , Feil , C M , Nieger , M & Gudat , D 2021 , ' Synthesis and Thermally and Light Driven Cleavage of an N-Heterocyclic Diphosphine with Inorganic Backbone ' , Zeitschrift für anorganische und allgemeine Chemie , vol. 647 , no. 4 , pp. 279-285 . https://doi.org/10.1002/zaac.202000252

http://hdl.handle.net/10138/327138
https://doi.org/10.1002/zaac.202000252

Journal of Inorganic and General Chemistry
ZAAC
Zeitschrift für anorganische und allgemeine Chemie
DOI: 10.1002/zaac.202000252
ARTICLE

Synthesis and Thermally and Light Driven Cleavage of an N-Heterocyclic Diphosphine with Inorganic Backbone

Markus Blum,[a] Christoph M. Feil,[a] Martin Nieger,[b] and Dietrich Gudat*[a]

Dedicated to Professor Dr. Thomas M. Klapötke on the Occasion of his 60th Birthday

Abstract. A diphosphine with an unsupported PP bond connecting two carbon-free "inorganic" 1,3,2,4,5-diazaphosphadisilolidine rings was prepared by reductive coupling of a P-chloro-substituted monocyclic precursor molecule. VT-EPR studies revealed that the diphosphine exists in solution, like other compounds of this kind, in dynamic equilibrium with the corresponding phosphinyl radicals. Determination of the radical concentration from the EPR spectra permitted to calculate thermochemical parameters for the homolytic PP bond fission. The results disclose that both the enthalpy and entropy of dissociation are higher than in topologically related bi(diazaphospholidines). The impact of the entropy term allows explaining that, regardless of the presence of an energetically rather stable PP bond, the onset of dissociation is observable even at ambient temperature. Irradiation experiments showed that radical formation cannot only be induced thermally, but also by photolysis.

Introduction

Phosphinyl radicals are divalent phosphorus compounds of general composition $R_2P^{\bullet}$ that are distinguished by an open shell electron structure with a formal 7 VE electron configuration. Known examples span the whole range from transient species, which occur merely as short-lived reaction intermediates (e.g. $H_2P^{\bullet}$),[1] over persistent radicals that possess extended life times in condensed phase and are easily detected spectroscopically,[2] to thermally stable compounds that can be isolated in crystalline form.[3] The creation of long-lived phosphinyl radicals can be accomplished by different routes. Reduction of chlorophosphine precursors enabled the generation of the first persistent phosphinyl radicals **1a**,**b** (Scheme 1) by the group of *Lappert* in 1976,[4] and was also employed by the groups of *Cummins*,[5] *Bertrand*,[6] and *Ishida* and *Iwamoto*[7] in their syntheses of the isolable crystalline radicals **2**–**4**. Of these species, **2** and **3** benefit from electronic stabilization by two transition metal imido or guanidinato moieties, respectively, while **4** is considered an electronically unperturbed radical that owes its existence exclusively to kinetic stabilization by steric effects. It should be noted that a complementary oxidative approach was used to prepare an isolable phosphinyl radical cation with a positive charge residing on an adjacent iminium unit.[8]

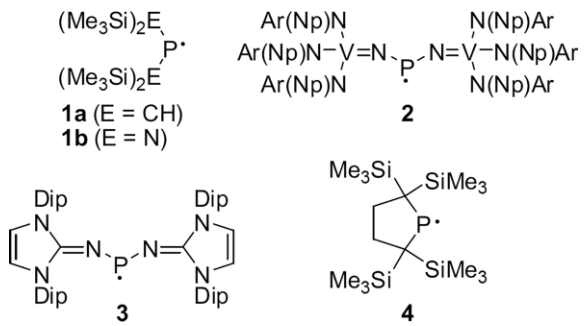

Scheme 1. Molecular structures of persistent (**1a**,**b**) or isolable (**2**–**4**) phosphinyl radicals (Np = *neo*-pentyl, Ar = 3,5-dimethylphenyl, Dip = 2,6-diisopropylphenyl).

An alternative to radical generation via redox processes is the homolytic fission of the PP bond of diphosphines $\{\mathbf{5}\}_2$ or $\{\mathbf{6}\}_2$, respectively. This process is usually initiated by thermal activation, and fission products **5**, **6** and their precursors exist usually in a temperature dependent equilibrium (Scheme 2).[9]

The prevalence of the dimers at low temperature and in the solid state indicates radicals **1a**,[10] **5**, **6** to be, unlike **2**–**4**, thermodynamically unstable towards dimerization. We have some time ago confirmed and quantified this conjecture by experimentally determining thermochemical data for the bond fission reaction.[9e,11]

Interpretation of these data with the help of computational studies suggested that the stabilization of phosphinyl radicals is predominantly steric in origin, while electronic effects seemed to have only minor impact. In accord with an earlier postulate derived from theoretical models,[10] the experimental

* Prof. Dr. Dr. h.c. Dietrich Gudat
E-Mail: gudat@iac.uni-stuttgart.de
[a] Institut für Anorganische Chemie
Universität Stuttgart
Pfaffenwaldring 55
70550 Stuttgart, Germany
[b] Department of Chemistry
University of Helsinki
P.O Box 55
00014 University of Helsinki, Finland
Supporting information for this article is available on the WWW under **http://dx.doi.org/10.1002/zaac.202000252** or from the author.

{5-7}$_2$ 5-7

	R	R'	Ref.
5a	*i*Pr$_2$N	(Me$_3$Si)$_2$N	
5b	*i*Pr$_2$N	2,6-(F$_3$C)$_2$C$_6$H$_3$	
5c	*i*Pr$_2$N	*i*Pr$_2$N	
5d	*i*Pr$_2$N	TMP	
6a	-N(Dip)-CH=CH-N(Dip)-		
6b	-N(Dip)-CH$_2$CH$_2$-N(Dip)-		
6c	-N(Ar')-CH$_2$CH$_2$-N(Ar')-		
6d	-N(*t*Bu)-CH$_2$CH$_2$-N(*t*Bu)-		
7	-N(*t*Bu)-SiMe$_2$SiMe$_2$-N(*t*Bu)-		

Scheme 2. Formation of phosphinyl radicals by thermally induced fission of diphosphines (TMP = 2,2,6,6-tetramethylpiperidinyl, Dip = 2,6-diisopropylphenyl, Ar′ = 2-*tert*-butylphenyl).

data corroborated that radical formation is facilitated when the dimers are loaded with strain energy that can be discharged upon bond fission. A considerable fraction of this strain energy is attributed to unfavorable distortions of bond and torsional angles that are enforced by a high degree of steric congestion in the overcrowded dimer and can be healed by structural relaxation of the sterically more flexible free radical.[10,11] A closer inspection revealed, however, that the situation is more complicated as bulky substituents may not only favor radical formation, but can also contribute to the stabilization of the dimers by dispersion forces.[11,12] Due to the action of many variables, a concise and detailed understanding of the factors governing the energetic and entropic contributions to radical stabilization is yet out of reach, and further studies are needed. Cyclic radicals still seem a viable entry point as their higher conformational rigidity is expected to facilitate insight. Following this rationale, we report here on a study of the PP bond fission of bis-heterocyclic diphosphine {**7**}$_2$ (Scheme 2) featuring a carbon-free, purely "inorganic" cyclic backbone. The molecular structure relates topologically to those of bi(diazaphospholidines) **6b**–**6d**, but formal replacement of the ethanediyl moiety by a larger and less flexible Si$_2$Me$_4$ unit is expected to provide for angular distortions and conformational preferences that differ from those of **6b**–**6d**. Moreover, we established for the first time that irradiation with UV-light can induce an isothermal shift of the radical/diphosphine equilibrium to generate a photo-stationary state characterized by an increased radical concentration.

Results and Discussion

Syntheses

As a precursor to diphosphine {**7**}$_2$, we first synthesized previously known chlorophosphine **8**[13] following a reported two-step procedure involving double amination of 1,2-dichloro-1,1,2,2-tetramethyl disilane with *tert*-butylamine[14] and subsequent ring closure with phosphorus trichloride. Formation of the diphosphine was then accomplished by reductive coupling of **8** with magnesium in THF, using sonication in an ultrasound bath to activate the metal (Scheme 3). Work-up afforded a moderate yield of crystalline product, which was identified by spectroscopic and analytical data. Both **8** (the crystal structure of which was previously unknown) and {**7**}$_2$ were further characterized by single-crystal X-ray diffraction studies.

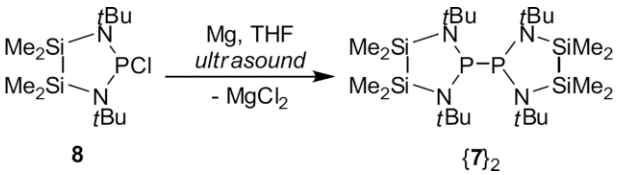

8 {**7**}$_2$

Scheme 3. Synthesis of {**7**}$_2$.

Crystallographic Studies

The availability of crystallographic data for **8** (Figure 1) and 2-thiocyanato-1,3-di-*tert*-butyl-4,4,5,5-tetramethyl-1,3,2,4,5-diazaphosphadisilolidine (**9**)[15] (Scheme 4) permitted comparing the structural features of the heterocyclic rings in the sterically strained dimer {**7**}$_2$ (Figure 2) and the less strained monocyclic "molecular halves". Inspection of selected metric parameters (Table 1) reveals that the Si–Si and Si–N distances in all compounds are essentially indistinguishable within experimental error. The P–N distances in the dimer are slightly elongated by some 0.06 Å, but similar effects occur also in monocyclic diazaphospholenes and diazaphospholidines and are attributable to the modulation of hyperconjugation between the nitrogen lone-pairs and the various exocyclic P–X bonds rather than steric effects.[16] We conclude therefore, that any steric strain associated with the formation of the dimeric struc-

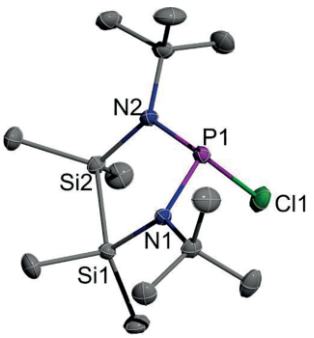

Figure 1. Representation of the molecular structure of **8** in the crystal. Hydrogen atoms are omitted for clarity. Thermal ellipsoids are drawn at the 50 % probability level. Selected distances and angles are listed in Table 1.

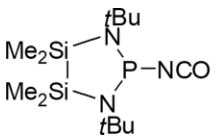

9

Scheme 4. Molecular structure of **9**.

Table 1. Selected distances /Å and angles /° for $\{7\}_2$, **8**, **9**.

	8	**9** [a]	$\{7\}_2$	
P–N	1.6764(8)	1.679(3)	1.7363(10)	1.7361(10)
	1.6825(8)	1.683(3)	1.7418(10)	1.7452(10)
N–Si	1.7665(8)	1.764(3)	1.7576(10)	1.7579(10)
	1.7689(8)	1.769(3)	1.7712(10)	1.7721(10)
Si–Si	2.3223(4)	2.3390(12)	2.3166(5)	2.3178(5)
P–X	2.2188(4)	1.814(3)	2.3034(4)	
N–P–N	103.86(4)	104.42(13)	104.29(5)	104.18(5)
N–P–X [b]	100.45(3)	98.56(13)	97.83(4)	97.65(4)
	100.51(3)	99.49(13)	105.21(4)	106.18(4)
Σ(X–P–Y) [c]	304.82(10)	302.47(39)	307.33(13)	308.01(13)
Σ(X–N–Y) [c]	357.70(16)	358.9(5)	355.5(2)	355.3(2)
	358.10(16)	359.7(5)	355.8(2)	356.3(2)

a) Data from reference[15]. b) X = Cl (**8**), N (**9**), P ($\{7\}_2$). c) Sum of all bond angles at the central atom.

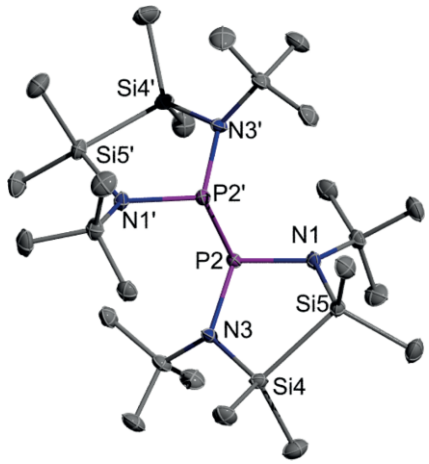

Figure 2. Representation of the molecular structure of $\{7\}_2$ in the crystal. Hydrogen atoms are omitted for clarity. Thermal ellipsoids are drawn at the 50% probability level. Selected distances and angles are listed in Table 1.

ture in $\{7\}_2$ leaves the bond lengths in the heterocycles untouched.

A similar invariance is also obvious for the endocyclic bond angles in the five-membered rings, whereas the pronounced asymmetry of the exocyclic N–P–P angles in $\{7\}_2$ (Table 1) gives a first indication for a sterically induced structural distortion in the dimer. Further angular variations, which tend to flatten the pyramidal coordination at the phosphorus and induce a slight pyramidalization of the coordination sphere around the nitrogen atoms, are too small to claim significance on their own account. However, in combination with additional warps in torsional angles, these deformations effect a clearly visible change from an envelope conformation of the five-membered rings with ecliptic alignment of the Me_2Si-units in the monomers **8**, **9** to a twist conformation with slightly staggered $SiMe_2$ moieties in $\{7\}_2$.

The *transoid* arrangement of the twisted five-membered rings of $\{7\}_2$ compares qualitatively to the features of topologically akin bi(diazaphospholidines) $\{$**6c**,**d**$\}_2$[9f,11] (see Scheme 2; note that crystalline $\{$**6b**$\}_2$[9d] exhibits gauche-conformation) containing two PP-connected C_2N_2P rings. The P–P distance in $\{7\}_2$ (2.3034(4) Å is by some 0.06 Å longer than in $\{$**6d**$\}_2$, which carries identical N-*t*Bu substituents, and lies in a similar range as in $\{$**6b**,**c**$\}_2$ where sterically more cumbersome N-aryl groups enforce some bond lengthening [P–P 2.270(2)–2.321(1) Å[11]]. Nitrogen coordination spheres are more or less pyramidalized in both $\{7\}_2$ and $\{$**6b-d**$\}_2$, but the deviation from planarity in bi(diazaphospholidines) [sum of bond angles range from 344.5(3)° to 359.8(4)°[11]] is more prominent than in $\{7\}_2$ [sum of bond angles 355.3(2) and 356.3(2)°]. Moreover, bi(diazaphospholidine) formation is not associated with a switch from envelope- to twist conformation of the heterocyclic ring that accompanies the conversion of **8** into $\{7\}_2$ (monocyclic diazaphospholidines prefer, like $\{$**6b-d**$\}_2$, twist conformation of the five-membered rings[9d,9f,11]). Even if these divergences reflect in part mere geometric factors (like the opening of the N–P–N angle in $\{7\}_2$, which is simply caused by the altered sizes of the ring atoms), they also imply that both heterocyclic frameworks give different responses to the increase in steric crowding associated with dimer formation.

Radical Generation

The formation of radicals through thermally induced PP bond homolysis was monitored by recording EPR spectra of a solution of $\{7\}_2$ in anhydrous and degassed toluene. As in case of bi(diazaphospholidines) $\{$**6b**,**c**$\}_2$ and acyclic tetraaminodiphosphines $\{$**5c**,**d**$\}_2$,[9d,11] an EPR signal (g = 2.0038) was already visible at ambient temperature (293 K) and increased steadily in intensity upon warming the solution up to a maximum temperature of 373 K. The signal displays a characteristic multiplet pattern arising from hyperfine coupling of the electron spin with the nuclear spins of phosphorus (^{31}P, I = ½), nitrogen (^{14}N, I = 1) and silicon (^{29}Si, I = ½, nat. abundance 4.6%) that is typical for diaminophosphinyl radicals and was analyzed by simulation of the spectrum recorded at 363 K (Figure 3). The magnitude of the hyperfine couplings to the phosphorus nucleus [a(^{31}P) = 75.4 G] is larger and that to the nitrogen nuclei [a(^{14}N) = 2.2 G] smaller than in diazaphospholidinyl radicals **6b**,**c** [a(^{31}P) = 60.9–63.8 G, a(^{14}N) = 3.7–4.3 G],[11] but the phosphorus hyperfine coupling matches the values reported for acyclic diaminophosphinyls [e.g. a(^{31}P) = 76.2 G (**5a**), 75.5 G (**5c**)[11]]. The observation of a signal multi-

plicity revealing hyperfine coupling of the electron spin in **7** with two equivalent ^{14}N nuclei indicates that the coordination planes of the phosphorus and both nitrogen atoms are, like in diazaphospholidinyls, close to coplanar. The observation of a significantly smaller ^{29}Si hyperfine coupling of 3.2 G than in **5a** [a(^{29}Si) = 12.2 G[11]] is attributable to a different orientational preference of the N–Si bond, which lies in the NPN plane in **7** (see below) and is nearly perpendicular in **5a**.[11]

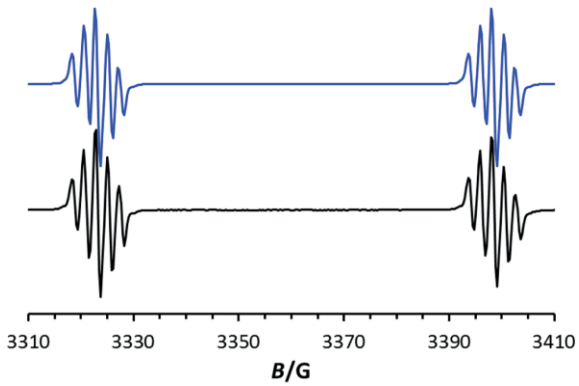

Figure 3. EPR spectrum of **7** at 363 K in toluene (black trace) and result of a simulation (blue trace). Simulation parameters: g = 2.0038, a(^{31}P) = 75.4 G, a(^{14}N) = 2.2 G, a(^{29}Si) = 3.2 G.

Because the changes in EPR signal intensity were fully reversible upon cooling, we conclude that radicals **7** and diphosphine $\{\mathbf{7}\}_2$ undergo, as in other reported cases,[9,11] reversible dynamic equilibration. Following a previously described procedure,[9e] we evaluated thermochemical parameters for the dissociation $\{\mathbf{7}\}_2 \rightleftarrows 2\ \mathbf{7}$ from the temperature dependent variation of the equilibrium constant $K = c(\mathbf{7})^2/c(\{\mathbf{7}\}_2)$ (see Figure 4).

The resulting value of ΔG_{Diss}^{295} of 90(5) kJ·mol^{-1}, which translates into an equilibrium exponent pK_{Diss}^{295} = 15.9(10) reveals that the equilibrium composition matches at ambient temperature roughly that observed for **6c**, but is further shifted to the side of the diphosphine than in **6b** (Table 2). It should be noted that similar Gibbs enthalpies of dissociation were also determined for acyclic tetraaminodiphosphines $\{\mathbf{5a}\}_2$ and $\{\mathbf{5d}\}_2$, whereas for the bi(diazaphospholidine) $\{\mathbf{6d}\}_2$ bearing identical N-substituents as $\{\mathbf{7}\}_2$ no thermally induced radical formation is reported. The substantially higher dissociation enthalpy ΔH_{Diss} of 135.2(26) kJ·mol^{-1} for $\{\mathbf{7}\}_2$ implies that PP bond homolysis is in this case energetically less favorable than in all reference compounds in Table 2, and it is only due to the compensation of the unfavorable energy term by

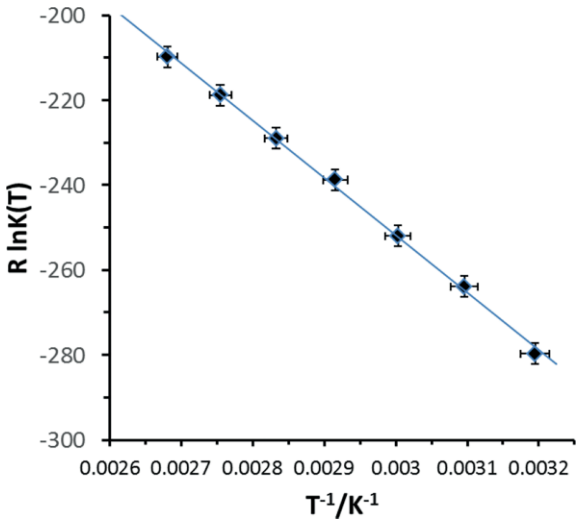

Figure 4. Van t′Hoff plot of $R\ \ln(K_{Diss}(T))$ vs. 1/T. Data points are represented as diamonds, and the straight line is the result of a linear regression analysis. ΔH_{Diss} = 135.2(26) kJ·mol^{-1} and ΔS_{Diss} = 154(8) J·(K·mol)$^{-1}$ were calculated from the slope and intersection of the regression line, respectively.

an unusually large positive entropy contribution [ΔS_{Diss} = 154(8) J·K^{-1}·mol^{-1}] that radical formation at ambient temperature is at all observable.

Having previously reported that bi(diazaphospholidines) and bi(diazaphospholenes) are also accessible by photolysis driven dehydrocoupling of secondary phosphine precursors,[17] we wanted to explore the feasibility of this route for the preparation of $\{\mathbf{7}\}_2$. The secondary phosphine $(Me_2Si(t\text{Bu})N)_2PH$ (**10**) was readily prepared by $LiBEt_3H$ reduction of **8** and identified by its NMR spectroscopic data.[18] Irradiation of a hexane solution of this species with a medium pressure mercury lamp produced indeed the expected target diphosphine $\{\mathbf{7}\}_2$, but the product was unstable under the reaction conditions and decomposed eventually into yet unidentified products, rendering this approach synthetically not useful. Attempting to monitor the photolysis reaction by EPR spectroscopy, we noted, however, that spectra of reaction mixtures containing $\{\mathbf{7}\}_2$ recorded under continuous UV irradiation displayed the EPR signal of **7**, which vanished when the irradiation source was turned off. Hypothesizing that radicals **7** may arise from a photochemical cleavage of $\{\mathbf{7}\}_2$, we recorded ambient temperature EPR spectra of a hexane solution of the pure dimer both under continuous UV irradiation (at a wavelength of 365 nm hitting the low energy tail of the first electronic transition of $\{\mathbf{7}\}_2$ cen-

Table 2. Experimental thermochemical data (free energy ΔG_{Diss}^{295} and equilibrium exponent pK^{295} at 295 K, reaction enthalpy ΔH_{Diss} and entropy ΔS_{Diss}) for the dissociation $R_2P–PR_2 \rightleftarrows 2\ R_2P^{\bullet}$, R_2P = **5a**, **5c**, **6b**, **6c**, **7**. Numbers in parentheses denote estimated standard deviations.

Diphosphine	ΔG_{Diss}^{295} a)	pK^{295} b)	ΔH_{Diss} a)	ΔS_{Diss} c)	Reference
$\{\mathbf{5a}\}_2$	69.6(28)	12.3(5)	95.4(14)	87(5)	[11]
$\{\mathbf{5c}\}_2$	70.2(21)	12.4(4)	108.9(12)	131(4)	[11]
$\{\mathbf{6b}\}_2$	69.4(21)	12.3(22)	102.3(11)	112(4)	[11]
$\{\mathbf{6c}\}_2$	88.6(17)	15.7(28)	104.9(10)	55(3)	[11]
$\{\mathbf{7}\}_2$	90(5)	15.9(10)	135.2(26)	154(8)	this work

a) In kJ·mol^{-1}. b) $pK^{295} = -\log(K_{Diss}^{295})$. c) In J·K^{-1}·mol^{-1}.

tered at 304 nm) and in the dark. The outcome of this study revealed that the intensity of the EPR signal increases indeed significantly when the spectrum is recorded under continuous irradiation (Figure 5a). Time dependent monitoring of the EPR signal discloses that the raise in intensity comes abruptly when the irradiation is switched on, and then slowly adjusts to a new equilibrium level. Switching the light off immediately re-establishes the original signal strength (Figure 5b, c). Similar results were also obtained with a sample of $\{\mathbf{5c}\}_2$ (see Supporting Information).

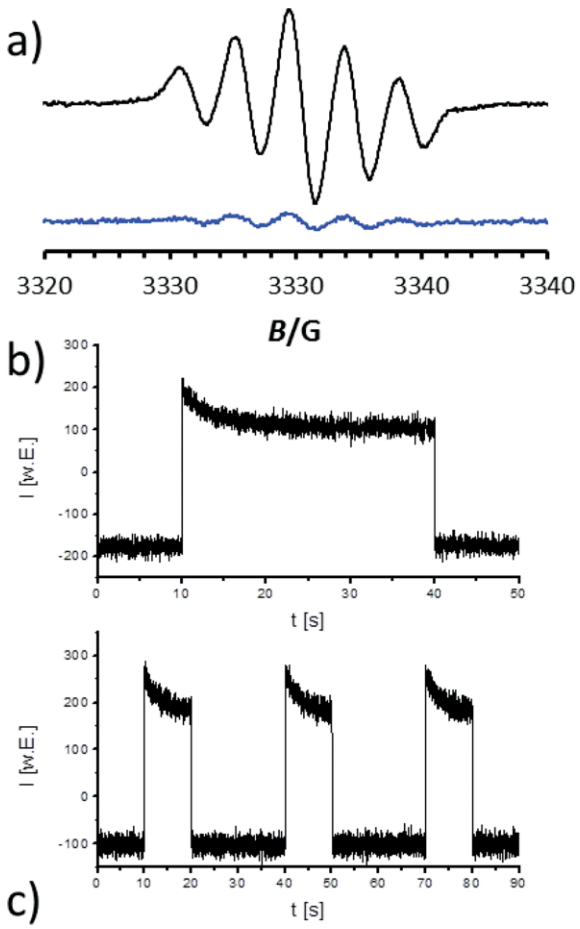

Figure 5. (a) Expansion of the low field multiplet component in EPR spectra of a hexane solution of $\{\mathbf{7}\}_2$ recorded at 298 K without (blue trace) and with (black trace) continuous UV-irradiation at 386 nm. (b) Time dependence of the signal strength at a fixed magnetic field of 3330.2 G. UV-irradiation at 386 nm was switched on 10 sec and switched off 40 sec after the measurement had been started. (c) Monitoring the signal strength as in (b) during three consecutive cycles with 10 sec irradiation periods. Vertical axes represent arbitrary units.

We attribute the incidental raise in signal intensity to a shift in the thermal equilibrium composition caused by formation of an excess concentration of radicals via photochemically induced PP bond homolysis. The excess radical concentration is maintained as long as the light source is on, but returns back to the thermal equilibrium value when it is switched off. The immediate restitution of the original equilibrium concentration implies that the surplus radicals recombine at a rate faster than the time resolution of the instrument. The non-equilibrium radical concentration level reached during the irradiation period must then be considered a photo-stationary state in which the thermal balance between radical formation and annihilation is disturbed by the generation of excess radicals through the photolysis process. The slow decay of the radical concentration during the early stage of the irradiation period is less well understood. We hypothesize that this phenomenon is possibly connected with the dissipation of the recombination energy produced by the excess radicals, which may accelerate radical recombination due to local heating until a new, stable temperature gradient in the sample is reached. It should be noted that the generation of phosphinyl radicals by UV-induced reduction of chlorophosphine precursors with electron rich olefins is known,[4,9b,19] but a light driven shift of PP-bond homolysis equilibria is to the best of our knowledge unprecedented.

Computational Studies

DFT calculations on radical **7** and diphosphine $\{\mathbf{7}\}_2$ were carried out at the ωB97x-D/cc-pVDZ level of theory that had already been employed in earlier studies on radicals **5**, **6**.[11] The subsequent discussion is based on molecular geometries of **7** and $\{\mathbf{7}\}_2$ that were obtained by energy optimization using the solid-state structures of **8** and $\{\mathbf{7}\}_2$ as starting points, and established as local minima on the energy hypersurface by frequency calculations. Computed and experimental molecular structures of $\{\mathbf{7}\}_2$ are in good agreement, and the computations succeed in particular in the critical prediction of the P–P distance, yielding a value of 2.297 Å that is very close to the experimental result of 2.3034(4) Å. The computed molecular structure of radical **7** is characterized by an essentially planar conformation of the heterocycle and an eclipsed alignment of the methyl substituents in 4,5-position.

Computation of the magnetic properties of radical **7** yields values of 85.7 G and 3.5 G for the hyperfine couplings a(^{31}P) and a(^{14}N). Even if these figures lie somewhat above the experimental data, they are a good match to the values computed for **5**, **6**,[11] where a very similar overestimation of the experimental data was achieved, and must be considered quite reasonable results in view of the fact that no conformational averaging was performed. The localization of 77 % and 20 % of the computed spin density on the *p* orbitals of the phosphorus and the nitrogen atoms, respectively, reproduces the results obtained on **5b**,**c** and reveals that the modification in the heterocyclic backbone leaves the electronic structure of the radical unaffected.

While the computational model is known to fail in reproducing quantitatively the energetics of the dissociation,[11] comparison of calculated dissociation enthalpies for $\{\mathbf{7}\}_2$ (163.2 kJ·mol^{-1}) and bi(diazaphospholidines) $\{\mathbf{6b}\}_2$ (158.4 kJ·mol^{-1})[11] and $\{\mathbf{6c}\}_2$ (157.4 kJ·mol^{-1})[11] confirms that PP bond fission in the former is expected to be slightly more endoergic, even if the observed difference is underestimated. Moreover, as had been noted before, the variation in entropy contributions is not reproduced very well, and a reliable analysis of the impact of steric factors on the dissociation energetic values is thus currently unfeasible.

Conclusions

A newly synthesized bi(diazaphosphadisilolidine) possesses a molecular shape which qualitatively resembles that of an analogous bi(diazaphospholidine), but features an elongated P–P bond that readily undergoes homolytic fission with formation of diazaphosphadisilolidine radicals. Even if the bond breaking process is more endoergic than in sterically encumbered bi(diazaphospholidines) with comparable P–P distances, a high entropy contribution provides for the generation of a spectroscopically detectable amount of radicals even at ambient temperature. For the first time, diphosphine homolysis was initiated not only by thermal activation but also by photolysis.

Experimental Section

All manipulations were carried out in an atmosphere of dry argon or nitrogen using standard vacuum line techniques or in glove boxes. Solvents were dried prior to use by common procedures. NMR spectra were recorded at 303 K on Bruker Avance 400 (^{1}H 400.1 MHz, ^{31}P 161.9 MHz, ^{29}Si 79.49 MHz) or Avance 250 (^{1}H 250.1 MHz, ^{31}P 101.2 MHz) spectrometers. ^{1}H NMR chemical shifts were referenced to TMS using the signals of the residual protons or carbon atoms of the deuterated solvent [^{1}H: $\delta(CDCl_3)$ = 7.24, $\delta(CD_2Cl_2)$ = 5.32, $\delta([D_6]DMSO)$ = 2.50] as secondary references. ^{31}P and ^{29}Si NMR chemical shifts were referenced using the Ξ-scale[20] with 85 % H_3PO_4 (Ξ = 40.480747 MHz, ^{31}P) and TMS (Ξ = 19.867187 MHz, ^{29}Si) as secondary reference. Coupling constants are given as absolute values. Elemental analyses were obtained with an Elementar Micro Cube elemental analyzer. UV/Vis spectra were recorded with a J&M TIDAS spectrophotometer. The synthesis of 1,2-di-*tert*-butylamino-1,1,2,2-tetramethyldisilane was carried out as described.[14]

Crystal Structure Determinations: Single-crystal X-ray diffraction data were collected on a Bruker Kappa APEX II Duo diffractometer equipped with a KRYO-FLEX cooling device at 135(2) K for **8** and on a Bruker D8 VENTURE with Photon100 detector at 123(2) K for $\{\mathbf{7}\}_2$ using Mo-K_α radiation (λ = 0.71073 Å) for both samples. Crystals were selected under Paratone-N oil, mounted on nylon loops, and immediately placed in a cold stream of N_2. The structures were solved by direct methods (SHELXS-2014)[21] and refined with a full-matrix least-squares Scheme on F^2 (SHELXL-2014).[21] Semi-empirical absorption corrections from equivalents were applied. Non-hydrogen atoms were refined anisotropically. Further crystallographic data and details on the structure solution are given in the Supporting Information.

Crystallographic data (excluding structure factors) for the structures in this paper have been deposited with the Cambridge Crystallographic Data Centre, CCDC, 12 Union Road, Cambridge CB21EZ, UK. Copies of the data can be obtained free of charge on quoting the depository numbers CCDC-2011917 ($\{\mathbf{7}\}_2$) and CCDC-2011943 (**8**) (Fax: +44-1223-336-033; E-Mail: deposit@ccdc.cam.ac.uk, http://www.ccdc.cam.ac.uk).

EPR Studies: VT-EPR spectra were measured with a Bruker EMX X-band spectrometer. Quantitative EPR measurements and evaluation of thermochemical data from the spectroscopic data were carried out using the same protocol that had been applied in case of $\{\mathbf{6a–c}\}_2$. The experiments were conducted with a 10(1) mM solution of $\{\mathbf{7}\}_2$ in degassed, anhydrous toluene using a calibrated ultramarine sample as reference. A detailed description of the procedure employed has been given elsewhere.[9e,11] EPR-spectra under UV-irradiation were recorded at 298 K on a Magnettech MiniScope MS5000 spectrometer equipped with an optical irradiation unit operating at a wavelength of 365 nm. Hyperfine splitting was determined by spectral simulation with EasySpin.[22]

Computational Studies were carried out with the Gaussian09 suite of programs.[23] For compatibility with previous studies, calculations on isolated molecules (in the gas phase) were performed with the ωB97X-D functional[24] and a cc-pVDZ basis set,[25] using an ultrafine grid for numerical integrations. Molecular structures of **7** and $\{\mathbf{7}\}_2$ were first energy optimized without symmetry constraints using the XRD data of $\{\mathbf{7}\}_2$ and **8** as starting points. Harmonic frequencies were calculated at the same level and allowed us to identify the optimized gas phase structures as local minima (only positive eigenvalues of the Hessian matrix) on the potential energy surface. Energies (including vibrational zero-point energy (ZPE) correction), enthalpies, and free enthalpies calculated for the dissociation reactions are corrected for basis set superposition errors (BSSE), the necessary corrections being obtained by counterpoise calculations.

2-Chloro-1,3-di-*tert*-butyl-3,3,4,4-tetramethyl-1,3,2,4,5-diazaphosphadisilolidine (8): *n*-Butyllithium (6.0 mL of a 2.5 M solution in hexane, 15.0 mmol) was added dropwise at –78 °C to a stirred solution of 1,2-di-*tert*-butylamino-1,1,2,2-tetramethyldisilane (1.80 g, 6.9 mmol) in Et_2O (50 mL). The mixture was stirred for further 30 min, while allowing it to warm to ambient temperature. After cooling again to –78 °C, PCl_3 (0.60 mL, 6.9 mmol) was added dropwise. After the addition was complete, the mixture was allowed to warm to room temperature and stirred for additional 18 h. The solvent was then evaporated under reduced pressure and the residue extracted with hexane. The hexane phase was filtered through Celite, and concentrated. Storage at –78 °C afforded **8** as a yellowish oily solid (yield 1.32 g, 59 %). Recrystallization from hexane at –78 °C afforded crystals suitable for X-ray diffraction. **^{31}P{^{1}H} NMR** ($CDCl_3$): δ = 213.4 (s). **^{1}H NMR** ($CDCl_3$): δ = 1.45 (d, $^4J_{PH}$ = 1 Hz, 18 H, *t*Bu), 0.52 (s, 6 H, $SiCH_3$), 0.38 (s, 6 H, $SiCH_3$). **^{13}C{^{1}H} NMR** ($CDCl_3$): δ = 58.3 (d, $^2J_{PC}$ = 28 Hz, NC), 33.0 (d, $^3J_{PC}$ = 14 Hz, CCH_3, 3.3 (br. s, $SiCH_3$); 2.6 (br. s, $SiCH_3$). **^{29}Si{^{1}H} NMR** ($CDCl_3$): δ = –2.3 (d, $^2J_{SiP}$ = 9 Hz, NSi). **UV/Vis** (hexane): λ_{max}/nm [ε_{max}/(L·mol^{-1}·cm^{-1})]: 264 (1.25×10^3), 304 (710). $C_{12}H_{30}N_2PSi_2$ (324.98 g·mol^{-1}): calcd. C 44.35 H 9.31 N 8.62 %; found C 44.16 H 9.39 N 8.50 %.

Bi-(1,3-di-*tert*-butyl-3,3,4,4-tetramethyl-1,3,2,4,5-diazaphosphadisilolidine) $\{\mathbf{7}\}_2$: Chlorophosphine **8** (1.32 g, 4.0 mmol) was dissolved in THF (20 mL). Magnesium turnings (approx. 240 mg, 10 mmol) were added and the mixture heated for 2 h to 48 °C under sonication with ultrasound. The solvent was then evaporated under reduced pressure and the residue extracted with hexane (20 mL). Solids were separated by filtration, the filtrate concentrated to a volume of 5–10 mL. Storage at –24 °C produced a crop of colorless crystals of 9 (yield 465 mg, 40 %). **^{31}P{^{1}H} NMR** ($CDCl_3$): δ = 122.3 (s). **^{1}H NMR** ($CDCl_3$): δ = 1.44 (s, 36 H, CCH_3), 0.55 (s, 12 H, $SiCH_3$), 0.42 (s, 12 H, $SiCH_3$). **^{13}C{^{1}H} NMR** ($CDCl_3$): δ = 56.1 (pseudo-t, 15 Hz, NC), 34.0 (pseudo-t, 6 Hz, CCH_3), 5.1 (br. s, $SiCH_3$), 4.4 (pseudo-t, 4 Hz, $SiCH_3$). **^{29}Si NMR** ($CDCl_3$): δ = –3.6 (pseudo-t, 4 Hz, NSi). $C_{24}H_{60}N_4P_2Si_4$ (579.06 g·mol^{-1}): calcd. C 49.78 H 10.44 N 9.68 %; found C 49.71 H 10.45 N 9.65 %.

Supporting Information (see footnote on the first page of this article): Crystallographic data for $\{\mathbf{7}\}_2$ and **8**, representations of EPR and NMR spectra, results of computational studies.

Acknowledgements

We thank *Dr. Brigitte Schwederski* and *Dr. Alexa Paretzki* for measuring EPR spectra, *Barbara Förtsch* for elemental analyses, *Nicholas Birchall* for UV/Vis spectra, and *Dr. Wolfgang Frey* (Institut für Organische Chemie) for collecting X-ray data sets. The computational studies were supported by the state of Baden-Württemberg through bwHPC and the German Research Foundation (DFG) through grant no INST 40/467–1 FUGG (JUSTUS cluster). Open access funding enabled and organized by Projekt DEAL.

Keywords: Phosphines; Radicals; Dimerization; Bond energy; Photolysis

References

[1] a) J. P. Ferris, R. Benson, *Nature* **1980**, *285*, 156–157; b) J. P. Ferris, R. Benson, *J. Am. Chem. Soc.* **1981**, *103*, 1922–1927; c) J. P. Ferris, A. Bossard, H. Kwaja, *J. Am. Chem. Soc.* **1984**, *106*, 318–324; d) J. Blazejowski, F. W. Lampe, *J. Phys. Chem.* **1981**, *85*, 1856–1864.

[2] For a review on this topic, see: P. P. Power, *Chem. Rev.* **2003**, *103*, 789–809.

[3] For a review, see: C. D. Martin, M. Soleilhavoup, G. Bertrand, *Chem. Sci.* **2013**, *4*, 3020–3030.

[4] M. J. S. Gynane, A. Hudson, M. F. Lappert, P. P. Power, H. J. Goldwhite, *J. Chem. Soc. Chem. Commun.* **1976**, 623–624.

[5] P. Agarwal, N. A. Piro, K. Meyer, P. Müller, C. C. Cummins, *Angew. Chem. Int. Ed.* **2007**, *46*, 3111–3114.

[6] O. Back, B. Donnadieu, M. von Hopffgarten, S. Klein, R. Tonner, G. Frenking, G. Bertrand, *Chem. Sci.* **2011**, *2*, 858–861.

[7] S. Ishida, F. Hirakawa, T. Iwamoto, *J. Am. Chem. Soc.* **2011**, *133*, 12968–12970.

[8] O. Back, M. A. Celik, G. Frenking, M. Melaimi, B. Donnadieu, G. Bertrand, *J. Am. Chem. Soc.* **2010**, *132*, 10262–10263.

[9] a) J.-P. Bezombes, P. B. Hitchcock, M. F. Lappert, J. E. Nycz, *Dalton Trans.* **2004**, 499–501; b) A. Dumitrescu, V. L. Rudzevich, V. D. Romanenko, A. Mari, W. W. Schoeller, D. Bourissou, G. Bertrand, *Inorg. Chem.* **2004**, *43*, 6546–6548; c) R. Edge, R. J. Less, E. J. L. McInnes, K. Müther, V. Naseri, J. M. Rawson, D. S. Wright, *Chem. Commun.* **2009**, 1691–1693; d) N. A. Giffin, A. D. Hendsbee, L. L. Roemmele, M. D. Lumsden, C. C. Pye, J. D. Masuda, *Inorg. Chem.* **2012**, *51*, 11837–11850; e) D. Förster, H. Dilger, F. Ehret, M. Nieger, D. Gudat, *Eur. J. Inorg. Chem.* **2012**, 3989–3994; f) O. Puntigam, D. Förster, N. A. Giffin, S. Burck, J. Bender, F. Ehret, A. D. Hendsbee, M. Nieger, J. D. Masuda, D. Gudat, *Eur. J. Inorg. Chem.* **2013**, 2041–2050.

[10] S. L. Hinchley, C. A. Morrison, D. W. H. Rankin, C. L. B. Macdonald, R. J. Wiacek, A. H. Cowley, M. F. Lappert, G. Gundersen, J. A. C. Clyburne, P. P. Power, *Chem. Commun.* **2000**, 2045; S. L. Hinchley, C. A. Morrison, D. W. H. Rankin, C. L. B. Macdonald, R. J. Wiacek, A. Voigt, A. H. Cowley, M. F. Lappert, G. Gundersen, J. A. C. Clyburne, P. P. Power, *J. Am. Chem. Soc.* **2001**, *123*, 9045.

[11] M. Blum, O. Puntigam, S. Plebst, F. Ehret, J. Bender, M. Nieger, D. Gudat, *Dalton Trans.* **2016**, *45*, 1987–1997.

[12] J.-D. Guo, S. Nagase, P. P. Power, *Organometallics* **2015**, *34*, 2028–2033.

[13] B. Wrackmeyer, J. Schiller, *Z. Naturforsch. B* **1992**, *47*, 662–667.

[14] W. R. Boon, *J. Chem. Soc.* **1947**, 307–318.

[15] M. Blum, J. Gebhardt, M. Papendick, S. H. Schlindwein, M. Nieger, D. Gudat, *Can. J. Chem.* **2018**, *96*, 549–554.

[16] a) D. Gudat, *Top. Heterocycl. Chem.* **2010**, *21*, 63–102; b) D. Gudat, *Acc. Chem. Res.* **2010**, *43*, 1307–1316.

[17] O. Puntigam, L. Könczöl, L. Nyulászi, D. Gudat, *Angew. Chem.* **2015**, *127*, 11730–11734; *Angew. Chem. Int. Ed.* **2015**, *54*, 11567–11571.

[18] A crude solid was isolated, but not analytically characterized. Spectroscopic data: $^{31}P\{^1H\}$ NMR (C_6D_6): δ = 59.0 s. ^1H NMR (C_6D_6): δ = 6.13 (d, $^1J_{PH}$ = 202 Hz, 1 H, PH), 1.32 (d, $^4J_{PH}$ = 1 Hz, 18 H, CCH_3), 0.35 (s, 6 H, $SiCH_3$), 0.29 (s, 6 H, $SiCH_3$). $^{13}C\{^1H\}$ NMR (C_6D_6): δ = 55.5 (d, $^2J_{PC}$ = 26 Hz, NC), 32.6 (d, $^3J_{PC}$ = 13 Hz, CH_3), 3.7 (d, $^2J_{PC}$ = 1 Hz $SiCH_3$), –2.7 (s, $SiCH_3$). $^{29}Si\{^1H\}$ NMR (C_6D_6): δ = –2.5 (d, $^2J_{SiP}$ = 10 Hz.

[19] M. J. S. Gynane, A. Hudson, M. F. Lappert, P. P. Power, H. Goldwhite, *J. Chem. Soc., Dalton Trans.* **1980**, 2428–2433.

[20] R. H. Harris, E. D. Becher, S. M. Cabral de Menezes, R. Goodfellow, P. Granger, *Concepts Magn. Reson.* **2002**, *14*, 326–346.

[21] G. M. Sheldrick, *Acta Crystallogr., Sect. A* **2008**, *64*, 112–122.

[22] a) S. Stoll, A. Schweiger, *J. Magn. Reson.* **2006**, *178*, 42–55; b) EasySpin 5.2.28, http://easyspin.org.

[23] Gaussian 09, Revision B01, M. J. Frisch, G. W. Trucks, H. B. Schlegel, G. E. Scuseria, M. A. Robb, J. R. Cheeseman, G. Scalmani, V. Barone, B. Mennucci, G. A. Petersson, H. Nakatsuji, M. Caricato, X. Li, H. P. Hratchian, A. F. Izmaylov, J. Bloino, G. Zheng, J. L. Sonnenberg, M. Hada, M. Ehara, K. Toyota, R. Fukuda, J. Hasegawa, M. Ishida, T. Nakajima, Y. Honda, O. Kitao, H. Nakai, T. Vreven, J. A. Montgomery Jr., J. E. Peralta, F. Ogliaro, M. Bearpark, J. J. Heyd, E. Brothers, K. N. Kudin, V. N. Staroverov, R. Kobayashi, J. Normand, K. Raghavachari, A. Rendell, J. C. Burant, S. S. Iyengar, J. Tomasi, M. Cossi, N. Rega, J. M. Millam, M. Klene, J. E. Knox, J. B. Cross, V. Bakken, C. Adamo, J. Jaramillo, R. Gomperts, R. E. Stratmann, O. Yazyev, A. J. Austin, R. Cammi, C. Pomelli, J. W. Ochterski, R. L. Martin, K. Morokuma, V. G. Zakrzewski, G. A. Voth, P. Salvador, J. J. Dannenberg, S. Dapprich, A. D. Daniels, Ö. Farkas, J. B. Foresman, J. V. Ortiz, J. Cioslowski, and D. J. Fox, Gaussian, Inc., Wallingford CT, **2009**.

[24] J.-D. Chai, M. Head-Gordon, *Phys. Chem. Chem. Phys.* **2008**, *10*, 6615–6620.

[25] a) T. H. Dunning, *J. Chem. Phys.* **1989**, *90*, 1007–1023; D. E. Woon, T. H. Dunning, *J. Chem. Phys.* **1993**, *98*, 1358–1371.

Received: July 1, 2020
Published Online: September 2, 2020